SUPPORTING INFORMATION

Heterotrimetallic synthetic approach in versatile functionalization of nanosized $\{M_xCu_{13-x}W_7\}^{3+}$ and $\{M_1Cu_8W_6\}$ (M = Co, Ni, Mn, Fe) metal–cyanide magnetic clusters

Michal Liberka,[a] Jedrzej Kobylarczyk,[a] Tadeusz Muziol,[b] Shin-ichi Ohkoshi,[c] Szymon Chorazy*[a,c] and Robert Podgajny*[a]

[a] Faculty of Chemistry, Jagiellonian University, Gronostajowa 2, 30-387 Kraków, Poland. [b] Department of Chemistry, School of Science, The University of Tokyo, 7-3-1 Hongo, Bunkyo-ku, Tokyo 113-0033, Japan.

*Corresponding authors: robert.podgajny@uj.edu.pl; chorazy@chemia.uj.edu.pl

Table S1. Results of SEM/EDXMA analysis of transition metal ions composition in **1**–**5**. (*part 1 of 3*)

metal	**Cu**	**W**	**Co**	**Ni**	**Mn**	**Fe**
compound 1						
measured atomic composition (only metals included, independent measurements)[a] / %	56.6(3.1)	39.1(1.5)	4.3(0.7)	-	-	-
	56.2(3.0)	39.2(1.5)	4.6(0.7)	-	-	-
	56.0(3.2)	39.6(2.8)	4.4(0.7)	-	-	-
	55.6(3.1)	40.1(1.6)	4.3(0.7)	-	-	-
	54.3(3.8)	39.5(1.9)	6.2(0.9)	-	-	-
	56.2(3.1)	37.3(1.6)	6.6(1.3)	-	-	-
	52.8(3.4)	42.9(1.7)	4.3(0.8)	-	-	-
	54.5(2.5)	40.3(2.2)	5.2(1.0)	-	-	-
	56.1(2.2)	38.3(2.9)	5.6(0.7)	-	-	-
average atomic composition (only metals included) / %	55.4(3.0)	39.5(2.0)	5.1(0.8)	-	-	-
relative atomic composition (only metals included, calculated for 8 W centers)	11.3(0.8)	8	1.1(0.2)	-	-	-
proposed metal composition	12	8	1	-	-	-
mass composition (only metals) / %	32.0(1.7)	65.2(3.3)	2.7(0.4)	-	-	-
mass composition (for full formula based on the proposed metal composition taking into account results of CHN) / %	**10.6(0.6)**	**21.6(1.1)**	**0.90(0.14)**	-	-	-
mass composition calculated for $Co_1Cu_{12}W_8C_{175}H_{354}N_{100}O_{48}$ / %	11.0	21.3	0.85	-	-	-
compound 2						
measured atomic composition (only metals included, independent measurements) / %	54.7(2.9)	38.8(2.5)	-	6.5(0.8)	-	-
	54.4(2.9)	38.2(2.6)	-	7.4(0.8)	-	-
	53.7(2.9)	38.7(1.5)	-	7.4(0.8)	-	-
	52.7(3.1)	39.6(2.7)	-	7.7(0.8)	-	-
	54.7(3.0)	37.4(2.6)	-	8.0(0.8)	-	-
	55.2(2.9)	37.9(2.6)	-	6.9(0.8)	-	-
	54.0(2.8)	39.0(1.5)	-	7.1(0.8)	-	-
	55.5(3.0)	37.5(2.7)	-	6.9(1.8)	-	-
	53.1(3.2)	40.0(1.6)	-	6.9(0.9)	-	-
average atomic composition (only metals included) / %	54.2(3.0)	38.6(2.3)	-	7.2(0.9)	-	-
relative atomic composition (only metals included, calculated for 8 W centers)	11.3(0.6)	8	-	1.5(0.2)	-	-
proposed metal composition	11.5	8	-	1.5	-	
mass composition (only metals) / %	31.4(1.7)	64.7(3.9)	-	3.86(0.48)	-	-
mass composition (for full formula based on the proposed metal composition taking into account results of CHN) / %	**10.4(0.6)**	**21.5(1.3)**	-	**1.28(0.16)**	-	-
mass composition calculated for $Ni_{1.5}Cu_{11.5}W_8C_{175}H_{354}N_{100}O_{48}$ / %	10.6	21.3	-	1.27	-	-

Table S1. Results of SEM/EDXMA analysis of transition metal ions composition in **1**–**5**. (*part 2 of 3*)

metal	**Cu**	**W**	**Co**	**Ni**	**Mn**	**Fe**
compound 3						
measured atomic composition (only metals included, independent measurements) / %	56.7(2.9)	38.0(2.6)	-	-	8.3(0.7)	-
	54.7(3.1)	39.2(2.7)	-	-	6.1(0.7)	-
	54.3(3.0)	38.8(2.6)	-	-	6.9(0.7)	-
	54.6(3.1)	38.8(2.8)	-	-	7.1(0.7)	-
	54.8(3.0)	38.3(2.6)	-	-	6.9(0.7)	-
	54.5(2.8)	38.2(1.5)	-	-	6.3(0.6)	-
	55.7(3.2)	37.6(2.8)	-	-	6.7(1.3)	-
	55.7(3.0)	38.9(2.7)	-	-	5.5(0.7)	-
average atomic composition (only metals included) / %	55.1(3.0)	38.5(2.5)	-	-	6.7(0.8)	-
relative atomic composition (only metals included, calculated for 8 W centers)	11.5(0.6)	**8**	-	-	1.4(0.2)	-
proposed metal composition	11.5	8	-	-	1.5	-
mass composition (only metals) / %	32.0(1.7)	64.7(4.2)	-	-	3.37(0.41)	-
mass composition (for full formula based on the proposed metal composition taking into account results of CHN) / %	**10.6(0.6)**	**21.4(1.4)**	-	-	**1.12(0.14)**	-
mass composition calculated for $Co_1Cu_{12}W_8C_{175}H_{354}N_{100}O_{48}$ / %	10.6	21.3	-	-	1.19	-
compound 4						
measured atomic composition (only metals included, independent measurements) / %	55.6(3.2)	37.1(2.8)	-	-	-	7.3(0.7)
	56.3(2.9)	36.1(2.5)	-	-	-	6.4(0.7)
	54.8(3.2)	37.6(2.8)	-	-	-	7.6(0.7)
	54.0(3.2)	38.7(1.6)	-	-	-	7.4(0.7)
	53.4(3.0)	40.1(1.6)	-	-	-	6.6(0.7)
	53.6(3.1)	38.0(2.7)	-	-	-	8.4(0.7)
	54.3(3.1)	39.3(1.6)	-	-	-	6.4(0.7)
	54.8(1.9)	38.2(1.6)	-	-	-	7.2(0.7)
average atomic composition (only metals included) / %	54.6(3.0)	38.1(2.2)	-	-	-	7.2(0.7)
relative atomic composition (only metals included, calculated for 8 W centers)	11.5(0.6)	8	-	-	-	1.5(0.2)
proposed metal composition	11.5	8	-	-	-	1.5
mass composition (only metals) / %	31.9(1.7)	64.4(3.7)	-	-	-	3.70(0.36)
mass composition (for full formula based on the proposed metal composition taking into account results of CHN) / %	**10.6(0.6)**	**21.3(1.2)**	-	-	-	**1.22(0.12)**
mass composition calculated for $Co_1Cu_{12}W_8C_{175}H_{354}N_{100}O_{48}$ / %	10.6	21.3	-	-	-	1.21

Table S1. Results of SEM/EDXMA analysis of transition metal ions composition in **1**–**5**. (*part 3 of 3*)

metal	**Cu**	**W**	**Co**	**Ni**	**Mn**	**Fe**
compound 5						
measured atomic composition (only metals included, independent measurements) / %	53.6(2.9)	39.3(1.5)	6.3(0.6)	-	-	-
	53.2(3.2)	39.9(1.5)	5.4(0.7)	-	-	-
	53.9(3.0)	40.4(2.8)	6.8(0.6)	-	-	-
	53.1(3.4)	39.4(1.6)	6.7(0.7)	-	-	-
	53.6(3.0)	38.3(1.9)	5.8(0.9)	-	-	-
	52.7(3.1)	41.1(1.6)	7.0(0.6)	-	-	-
	54.5(2.8)	37.2(1.7)	6.5(0.9)	-	-	-
	52.9(2.5)	40.1(2.2)	6.2(0.6)	-	-	-
	53.1(2.6)	38.0(2.9)	6.6(0.8)	-	-	-
average atomic composition (only metals included) / %	53.4(3.0)	39.3(2.0)	6.4(0.7)	-	-	-
relative atomic composition (only metals included, calculated for 6 W centers)	8.1(0.5)	6	1.0(0.1)	-	-	-
proposed metal composition	8	6	1	-	-	-
mass composition (only metals) / %	30.9(1.7)	65.7(3.3)	3.43(0.38)	-	-	-
mass composition (for full formula based on the proposed metal composition taking into account results of CHN) / %	**10.3(0.6)**	**21.9(1.1)**	**1.15(0.13)**	-	-	-
mass composition calculated for $Co_1Cu_{12}W_8C_{175}H_{354}N_{100}O_{48}$ / %	10.2	22.0	1.18	-	-	-

[a]For each compound, EDXMA (energy dispersive X-ray microanalysis) analyses were conducted on a few different single crystals and on a few places of the selected single crystal.

Comment to Table S1 – procedure for determination of atomic compositions of compounds 1–5

Atomic composition for metal centers embedded in the crystalline samples of **1**–**5** was measured using energy-dispersive X-ray microanalysis for a few representative crystals. The results of atomic compositions of W, Cu and a third metal center were averaged. The obtained average atomic compositions included only metals, and they were used to estimate the relative metal composition. It was calculated assuming 8 W-centers for compounds **1**–**4** and 6 W-centers for **5**, according to the crystal structures. The resulting relative atomic composition indicated the proposed metal composition of $\{Cu_{12}Co_1W_8\}$ in **1**, $\{Cu_{11.5}Ni_{1.5}W_8\}$ in **2**, $\{Cu_{11.5}Mn_{1.5}W_8\}$ in **3**, $\{Cu_{11.5}Fe_{1.5}W_8\}$ in **4**, and $\{Cu_8Co_1W_6\}$ in **5**. These proposed metal compositions were used to determine the full formula of the respective compounds, taking into account the results of CHN elemental analyses. We found that compounds **1**–**4** exhibit the identical solvent content of 44 water molecules and 3 MeOH molecules per $\{Cu_{13-x}M_xW_8\}$ unit while 31 water molecules and 5 MeOH molecules can be assigned to each $\{Cu_8Co_1W_6\}$ unit in **5** (please compare the results of CHN elemental analysis shown in Experimental section). Assuming these compositions, we could determine the experimental mass compositions for metals in the whole compounds. We used the average atomic composition which was firstly used to determent the mass composition for only metals, and, then, mass composition for metals including all non-metal atoms (C, H, N, O) of organic ligands, cyanides and solvent molecules. The resulting mass composition of metals for full formulas are shown in **bold** in Table S1. They were compared with the calculated mass composition for the proposed formulas, and a good agreement within the experimental error was found (see above). It confirmed the proposed formulas of all investigated compounds.

Table S2. Crystal data and structure refinement for **1** and **2** compared with the previously reported analogous $\{[Cu^{II}_{13}(Me_3tacn)_{12}(H_2O)][W^{IV}(CN)_8]_5[W^{V}(CN)_8]_2\}\cdot 24H_2O$ (**$Cu_{13}W_7$**) compound.

compound	**1**	**2**	**$Cu_{13}W_7$**
	this work	this work	*Inorg. Chem.*, 2010, **49**, 3101
empirical formula	$C_{172}H_{252}Co_1Cu_{12}N_{100}O_1W_8$	$C_{172}H_{252}Cu_{11.5}N_{100}Ni_{1.5}O_1W_8$	$C_{164}H_{302}Cu_{13}N_{92}O_{25}W_7$
formula weight	6028.93	6026.30	6076.01
T, K	100(2)	100(2)	291(2)
radiation	synchrotron (λ = 0.77538 Å)	synchrotron (λ = 0.77538 Å)	MoKα (λ = 0.71073 Å)
crystal system	orthorhombic	orthorhombic	tetragonal
space group	$P\ 2_12_12$ chiral	$P\ 2_12_12$ chiral	I 4mm non-centrosymmetric (non-chiral)
a, Å	32.2076(3)	32.3884(3)	31.2762(12)
b, Å	29.6713(4)	29.3119(5)	31.2762(12)
c, Å	16.1270(2)	16.0224(3)	16.1133(18)
α, β, γ, deg	90	90	90
V, Å^3	15411.6(3)	15211.1(4)	15762(2)
Z	2	2	2
ρ_{calc}, g/cm^3	1.299	1.316	1.280
qbs. coefficient, cm^{-1}	4.841	4.910	3.454
F(000)	5918	5919	6050
crystal type	dark violet needle	dark violet needle	blue block
crystal size, mm^3	0.13 × 0.06 × 0.03	0.11 × 0.05 × 0.03	0.28 × 0.22 × 0.20
θ range, deg	1.541 to 27.484	1.547 to 28.986	1.840 to 25.990
index range	$-35 \le h \le 38$, $-32 \le k \le 35$, $-19 \le l \le 19$	$-40 \le h \le 40$, $-36 \le k \le 35$, $-20 \le l \le 19$	$-38 \le h \le 31$, $-36 \le k \le 38$, $-19 \le l \le 19$
reflections collected	66555	74617	43299
independent reflections	26999	29846	8220
R_{int}	0.0581	0.0428	0.0768
completeness	0.998	0.972	0.998
data/restraints/ parameters	26999/368/1343	29846/835/1344	8220/1/511
goodness-of-fit on F^2	1.118	1.231	1.014
final R indices [I >=2σ(I)]	R_1 = 0.0838, wR_2 = 0.2383	R_1 = 0.0949, wR_2 = 0.2964	R_1 = 0.0532, wR_2 = 0.1097
R indices (all data)	R_1 = 0.0918, wR_2 = 0.2474	R_1 = 0.1058, wR_2 = 0.3080	R_1 = 0.0658, wR_2 = 0.1123
largest diff. peak/hole, e·Å^{-3}	3.727/–3.539	2.966/–3.521	1.727/–1.894
Flack parameter	0.022(9)	0.308(11)	0.010(11)

Table S3. Detailed structural parameters of 3d metal complexes in **1** and **2** compared with the previously reported analogous $\{[Cu^{II}_{13}(Me_3tacn)_{12}(H_2O)][W^{IV}(CN)_8]_5[W^{V}(CN)_8]_2\}\cdot 24H_2O$ (**$Cu_{13}W_7$**) compound.

parameter	**1**	**2**	**$Cu_{13}W_7$**
	this work (atom labels as in Fig. 1b and Fig. 3a)	this work (atom labels as in Fig. 1b and Fig. 3a)	*Inorg. Chem.*, 2010, **49**, 3101 (bond distances of the analogous complexes)
Co1/Ni1/Cu1–N2	2.27(3) Å	2.27(2) Å	Cu3, 2.297(10) Å
Co1/Ni1/Cu1–N82	2.23(2) Å	2.23(3) Å	2.251(9) Å
Co1/Ni1/Cu1–N12	2.049(19) Å	2.03(3) Å	2.000(6) Å
Co1/Ni1/Cu1–N21	2.00(2) Å	2.054(19) Å	2.000(6) Å
Co1/Ni1/Cu1–N81	2.195(18) Å	2.13(3) Å	2.113(6) Å
Co1/Ni1/Cu1–N83	2.12(2) Å	2.14(3) Å	2.113(6) Å
Co2/Ni2/Cu2–N13	2.21(2) Å	2.24(2) Å	Cu2,[a] 2.249(19) Å
Co2/Ni2/Cu2–N62	2.31(2) Å	2.33(4) Å	2.292(11) Å
Co2/Ni2/Cu2–N10	1.993(18) Å	2.00(2) Å	1.969(6) Å
Co2/Ni2/Cu2–N26	1.993(16) Å	2.05(2) Å	1.969(6) Å
Co2/Ni2/Cu2–N61	2.16(3) Å	2.05(4) Å	2.047(6) Å
Co2/Ni2/Cu2–N63	2.06(3) Å	2.15(4) Å	2.047(6) Å
Cu3–N1	2.42(2) Å	2.34(2) Å	Cu3, 2.297(10) Å
Cu3–N41	2.35(2) Å	2.31(3) Å	2.251(9) Å
Cu3–N6	1.972(18) Å	2.00(2) Å	2.000(6) Å
Cu3–N22	1.93(2) Å	1.98(2) Å	2.000(6) Å
Cu3–N42	2.132(19) Å	2.05(2) Å	2.113(6) Å
Cu3–N43	2.094(18) Å	2.08(2) Å	2.113(6) Å
Cu4–N5	1.951(15) Å	1.999(15) Å	Cu1, 1.947(9) Å
Cu4–N5’	1.951(15) Å	1.999(15) Å	1.947(9) Å
Cu4–N23	1.975(16) Å	1.98(2) Å	1.947(9) Å
Cu4–N23’	1.975(16) Å	1.98(2) Å	1.947(9) Å
Cu4–O1	2.30(3) Å	2.32(3) Å	2.365(16) Å
Cu5–N20	1.967(19) Å	2.05(3) Å	Cu4, 1.964(14) Å
Cu5–N27	1.939(19) Å	2.008(19) Å	1.930(7) Å
Cu5–N71	2.19(4) Å	2.21(5) Å	2.241(14) Å
Cu5–N72	2.03(3) Å	2.15(4) Å	1.998(13) Å
Cu5–N73	2.09(2) Å	2.14(4) Å	2.116(12) Å
Cu6–N7	1.981(19) Å	2.02(2) Å	Cu2,[a] 1.969(6) Å
Cu6–N24	1.979(16) Å	1.94(2) Å	1.969(6) Å
Cu6–N51	2.20(2) Å	2.21(4) Å	2.292(11) Å
Cu6–N52	2.10(3) Å	2.06(4) Å	2.047(6) Å
Cu6–N53	2.09(2) Å	2.09(4) Å	2.047(6) Å
Cu7–N11	1.972(18) Å	1.987(16) Å	Cu4, 1.930(7) Å
Cu7–N14	1.96(2) Å	1.98(2) Å	1.964(14) Å
Cu7–N91	2.18(3) Å	2.22(4) Å	2.241(14) Å
Cu7–N92	2.08(3) Å	2.21(4) Å	2.116(12) Å
Cu7–N93	2.06(3) Å	2.09(3) Å	1.998(13) Å

[a]Due to the symmetry and partial occupancies for the part of $\{Cu_{13}W_7\}$ cluster, Cu2 centre represents six- and five-coordinated complexes with half occupancies.

Table S4. Detailed structural parameters of $[W(CN)_8]^{n-}$ complexes in **1** and **2** compared with the previously reported analogous $\{[Cu^{II}_{13}(Me_3tacn)_{12}(H_2O)][W^{IV}(CN)_8]_5[W^{V}(CN)_8]_2\}\cdot 24H_2O$ (**Cu$_{13}$W$_7$**) compound.

parameter	**1**	**2**	**Cu$_{13}$W$_7$**
	this work	this work	*Inorg. Chem.*, 2010, **49**, 3101 (bond distances of the analogous complexes)
W1–C1	2.08(3) Å	2.18(3) Å	W2, 2.161(13) Å
W1–C2	2.15(3) Å	2.20(2) Å	2.188(11) Å
W1–C3	2.192(19) Å	2.19(4) Å	-
W1–C4	2.20(2) Å	2.12(2) Å	-
W2–C5	2.247(19) Å	2.14(3) Å	W1, 2.123(8) Å
W2–C6	2.15(2) Å	2.07(2) Å	2.137(11) Å
W2–C7	2.252(19) Å	2.25(3) Å	2.156(8) Å
W2–C8	2.17(3) Å	2.161(18) Å	2.160(8) Å
W2–C9	2.22(2) Å	2.09(3) Å	2.187(12) Å
W2–C10	2.210(18) Å	2.21(2) Å	-
W2–C11	2.15(2) Å	2.214(19) Å	-
W2–C12	2.145(18) Å	2.12(2) Å	-
W3–C13	2.08(3) Å	2.17(2) Å	W3, 2.13(2) Å
W3–C14	2.13(3) Å	2.23(3) Å	2.143(18) Å
W3–C15	2.15(2) Å	2.24(4) Å	2.18(2) Å
W3–C16	2.14(3) Å	2.10(2) Å	2.187(18) Å
W3–C17	2.23(2) Å	2.15(3) Å	2.192(17) Å
W3–C18	2.21(2) Å	2.19(2) Å	-
W3–C19	2.08(2) Å	2.14(3) Å	-
W3–C20	2.13(2) Å	2.17(2) Å	-
W4–C21	2.14(2) Å	2.20(3) Å	W1, 2.123(8) Å
W4–C22	2.158(18) Å	2.08(3) Å	2.137(11) Å
W4–C23	2.24(2) Å	2.232(14) Å	2.156(8) Å
W4–C24	2.213(16) Å	2.18(2) Å	2.160(8) Å
W4–C25	2.218(17) Å	2.25(3) Å	2.187(12) Å
W4–C26	2.225(16) Å	2.18(2) Å	-
W4–C27	2.15(3) Å	2.127(18) Å	-
W4–C28	2.14(2) Å	2.15(2) Å	-
W5–C29	2.19(2)	2.18(2) Å	-
W5–C30	2.156(19)	2.15(3) Å	-
W5–C31	2.19(2)	2.18(2) Å	-
W5–C32	2.15(2)	2.14(2) Å	-
W1–CN	173(2)° to 178(2)°	167(3)° to 175(2)°	179.5(11)° to 179.9(10)°
W2–CN	171.5(17)° to 179(2)°	167(3)° to 179(2)°	170.5(10)° to 177.9(7)°
W3–CN	172.7(18)° to 179(3)°	163(3)° to 177(2)°	171.6(14)° to 180(2)°
W4–CN	170.4(16)° to 180(2)°	164(2)° to 178(2)°	170.5(10)° to 177.9(7)°
W5–CN	163(3)° to 176(6)°	167(7)° to 176(4)°	-

Table S5. Results of Continuous Shape Measure (CSM) analysis for metal complexes in **1** and **2**.

compound, metal complex	CSM parameters[a]			geometry
six-coordinated metal complexes				
-	OC-6	TPR-6	-	-
1, $[Co1/Cu1(\mu\text{-}NC)_3(Me_3tacn)]^{-}$	0.533	15.249	-	OC-6
2, $[Ni1/Cu1(\mu\text{-}NC)_3(Me_3tacn)]^{-}$	0.512	15.199	-	OC-6
1, $[Co2/Cu2(\mu\text{-}NC)_3(Me_3tacn)]^{-}$	0.406	15.233	-	OC-6
2, $[Ni2/Cu2(\mu\text{-}NC)_3(Me_3tacn)]^{-}$	0.505	14.839	-	OC-6
1, $[Cu3(\mu\text{-}NC)_3(Me_3tacn)]^{-}$	0.406	15.233	-	OC-6
2, $[Cu3(\mu\text{-}NC)_3(Me_3tacn)]^{-}$	0.658	16.190	-	OC-6
five-coordinated metal complexes				
-	vOC-5	SPY-5	-	-
1, $[Cu4(\mu\text{-}NC)_4(H_2O)]^{2-}$	0.770	0.519	-	SPY-5
2, $[Cu4(\mu\text{-}NC)_4(H_2O)]^{2-}$	0.729	0.567	-	SPY-5
1, $[Cu5(\mu\text{-}NC)_2(Me_3tacn)]$	0.902	0.891	-	vOC-5/SPY-5
2, $[Cu5(\mu\text{-}NC)_2(Me_3tacn)]$	0.952	1.158	-	vOC-5/SPY-5
1, $[Cu6(\mu\text{-}NC)_2(Me_3tacn)]$	0.429	1.404	-	vOC-5
2, $[Cu6(\mu\text{-}NC)_2(Me_3tacn)]$	0.427	1.453	-	vOC-5
1, $[Cu7(\mu\text{-}NC)_2(Me_3tacn)]$	0.752	1.383		vOC-5
2, $[Cu7(\mu\text{-}NC)_2(Me_3tacn)]$	0.653	1.389		vOC-5
eight-coordinated metal complexes				
-	SAPR-8	TDD-8	BTPR-8	-
1, $[W1(CN)_8]^{n-}$	0.103	2.540	1.783	SAPR-8
2, $[W1(CN)_8]^{n-}$	0.179	2.347	2.209	SAPR-8
1, $[W2(CN)_8]^{n-}$	0.252	2.028	1.977	SAPR-8
2, $[W2(CN)_8]^{n-}$	0.440	2.153	2.307	SAPR-8
1, $[W3(CN)_8]^{n-}$	0.360	2.165	1.479	SAPR-8
2, $[W3(CN)_8]^{n-}$	0.343	2.254	1.828	SAPR-8
1, $[W4(CN)_8]^{n-}$	0.416	1.468	1.759	SAPR-8
2, $[W4(CN)_8]^{n-}$	0.637	1.426	1.632	SAPR-8
1, $[W5(CN)_8]^{n-}$	0.894	1.432	2.233	SAPR-8
2, $[W5(CN)_8]^{n-}$	0.407	2.433	2.328	SAPR-8

[a]CSM parameter represents the distortion from an ideal geometry. It equals 0 for an ideal polyhedron and increases with the increasing distortion. Polyhedrons used in calculations: OC-6 = parameter of an octahedron related to the O_h symmetry; TPR-6 = parameter of a trigonal prism related to the D_{3h} symmetry; vOC-5 = parameter of a vacant octahedron related to the C_{4v} symmetry; SPY-5 = parameter of a spherical square pyramid related to the D_{3h} symmetry; SAPR-8 = parameter of a square antiprism geometry related to the D_{4d} symmetry; TDD-8 = parameter of a triangular dodecahedron related to the D_{2d} symmetry; BTPR-8 = parameter of a bicapped trigonal prism related to the C_{2v} symmetry.

References: (*a*) M. Llunell, D. Casanova, J. Cirera, J. Bofill, P. Alemany, S. Alvarez, M. Pinsky and D. Avnir, *SHAPE v. 2.1. Program for the Calculation of Continuous Shape Measures of Polygonal and Polyhedral Molecular Fragments*, University of Barcelona: Barcelona, Spain, 2013; (*b*) D. Casanova, J. Cirera, M. Llunell, P. Alemany, D. Avnir and S. Alvarez, *J. Am. Chem. Soc*., 2004, **126**, 1755.

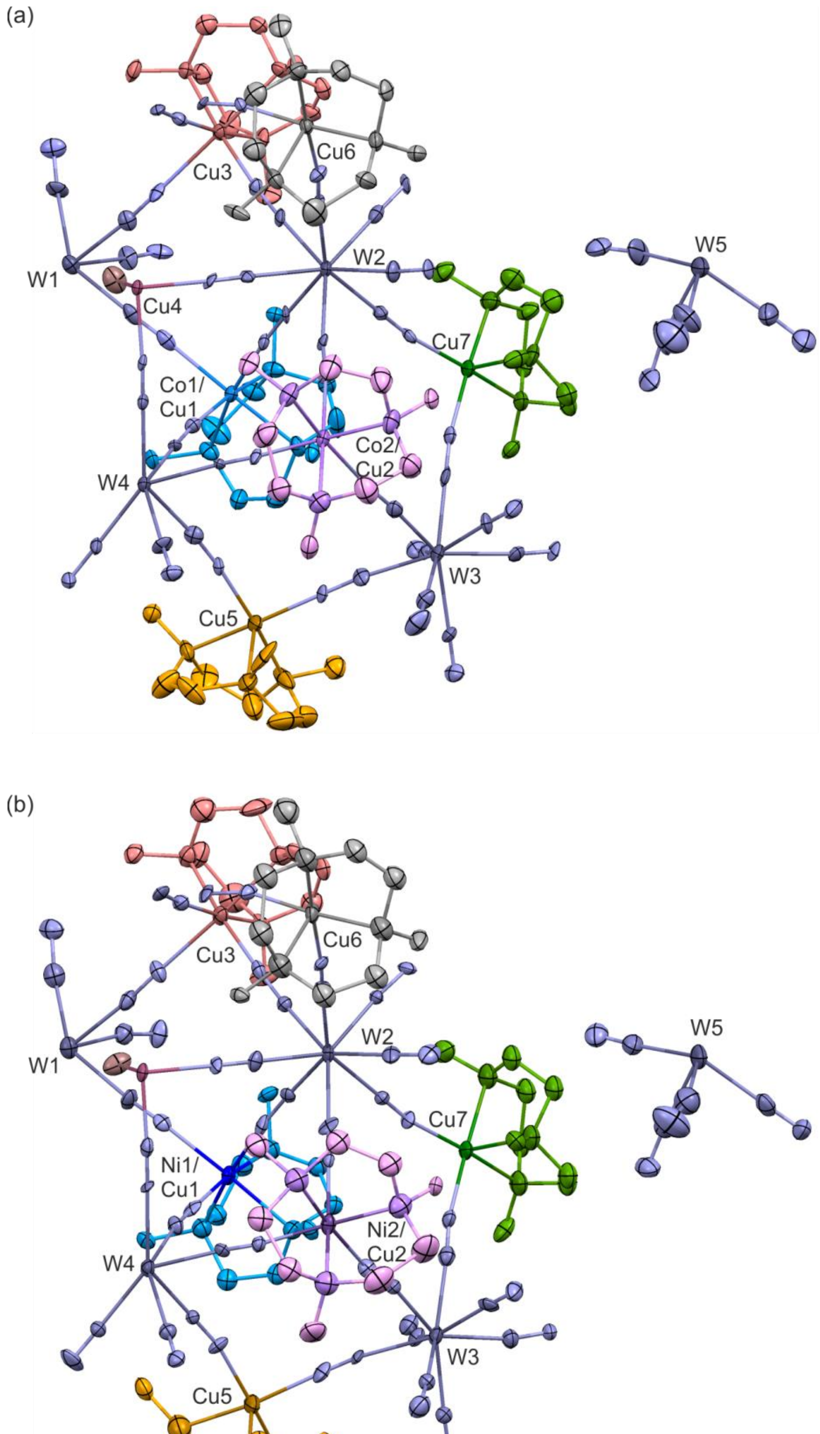

Figure S1. Comparison of the asymmetric units of **1** (*a*) and **2** (*b*) with the metal atoms labelling schemes. Thermal ellipsoids are presented at the 20% probability level. The detailed labelling scheme for the nitrogen atoms coordinated to Cu/Co metal centres in **1** is gathered in Figure 1b. The related bond lengths and angles are collected in Table S3. Hydrogen atoms are omitted for clarity.

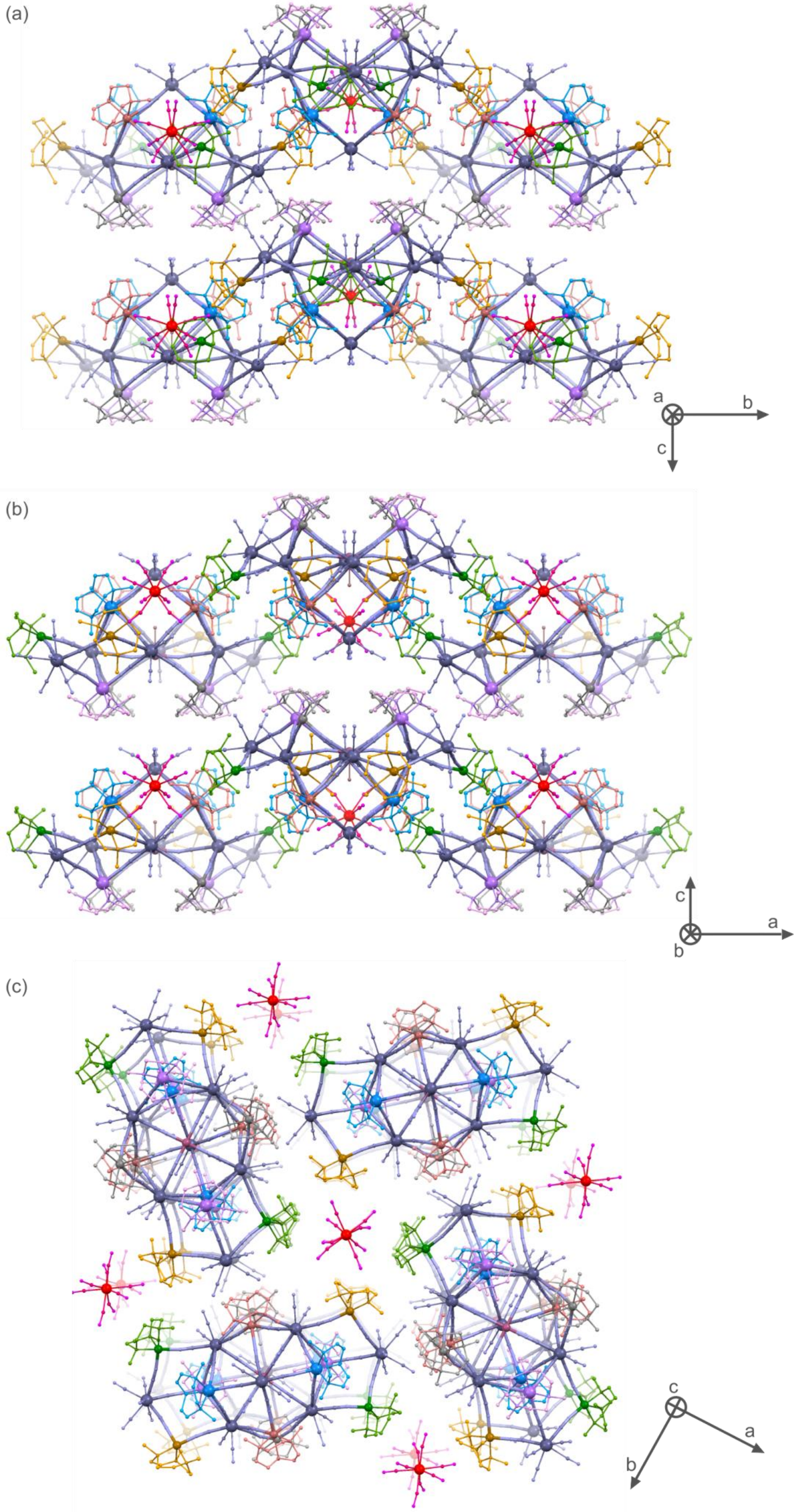

Figure S2. Views of the supramolecular network of **1** shown along the crystallographic ***a*** axis (a), ***b*** axis (b) and ***c*** axis (c). Atoms of clusters are coloured in the identical way as shown in Figure S1 while the non-coordinated $[W(CN)_8]^{3-}$ ions are shown in red–magenta colours.

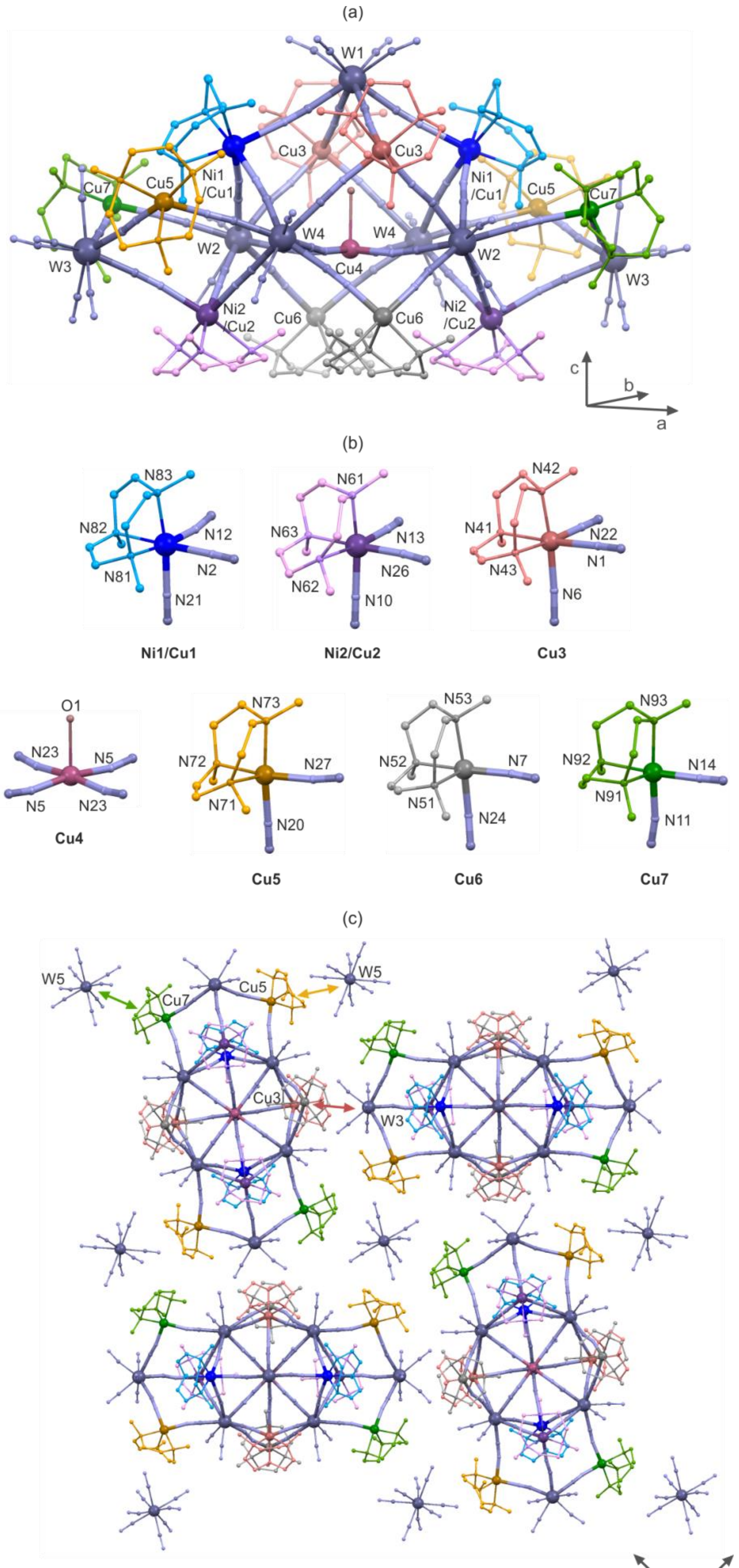

Figure S3. Crystal structure of **2**: views on the coordination skeleton of $\{Ni_{1.5}Cu_{11.5}W_7\}^{3+}$ clusters (a), detailed views on intracluster Ni and Cu complexes (b), and the supramolecular arrangement of clusters and uncoordinated $[W(CN)_8]^{3-}$ ions within *ab* crystallographic plane with the indication of the related shortest intermetallic contacts, Cu7–W5 of ca. 7.19 Å, Cu5–W5 of ca. 7.73 Å and Cu3–W3 of ca. 7.69 Å. Black arrows in (b) represent the axial elongation of the pseudo-octahedral 3d metal complexes.

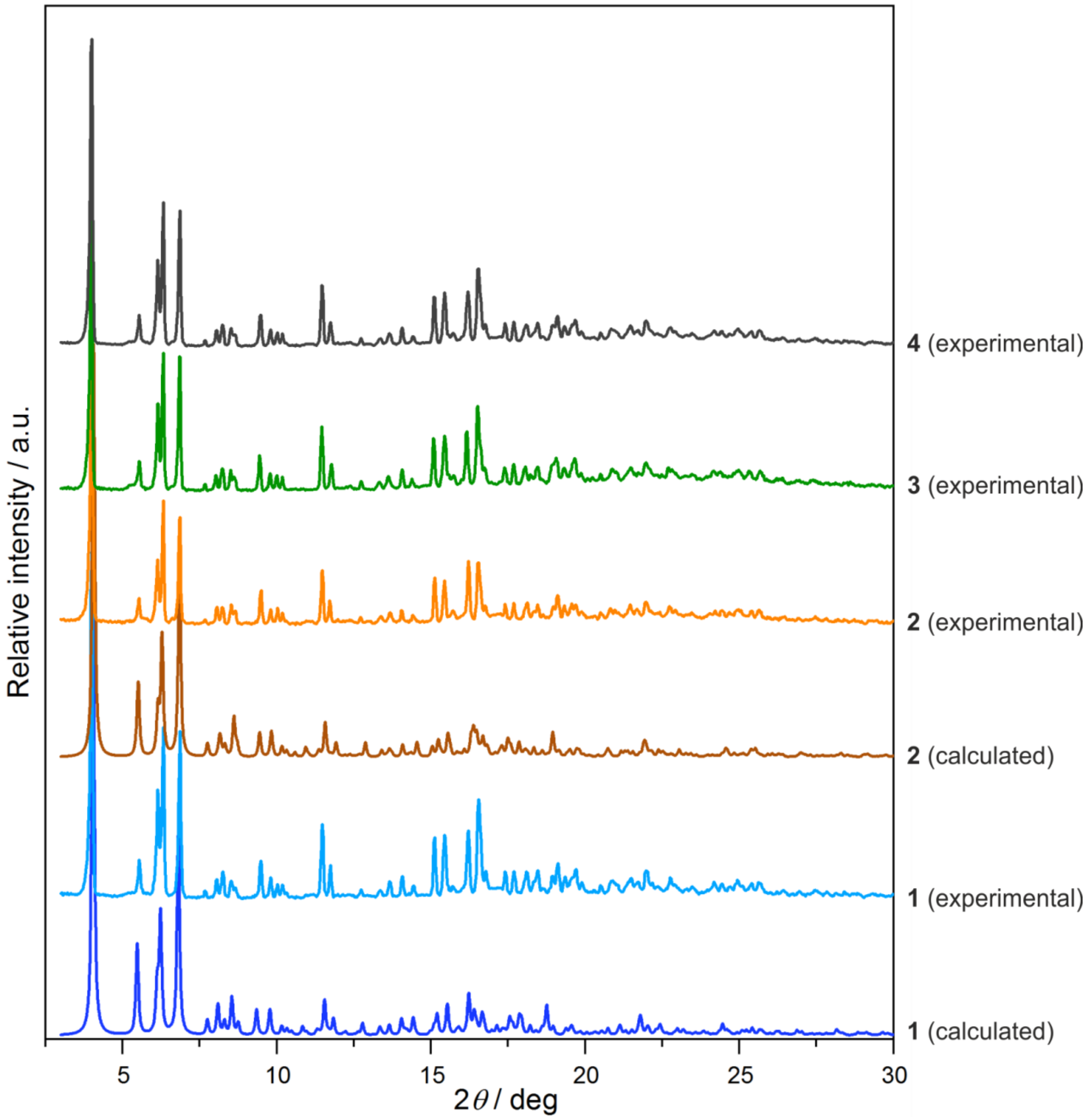

Figure S4. Experimental powder X-ray diffraction (PXRD) patterns of compounds **1**–**4** compared with the PXRD patterns calculated from the structural models of **1** and **2** obtained within the single-crystal X-ray diffraction structural analyses.

Table S6. Crystal data and structure refinement for **5** compared with the previously reported analogous $\{Cu^{II}[Cu^{II}(Me_3tacn)]_8[W^V(CN)_8]_6\}\cdot 5MeOH\cdot 31H_2O$ (**Cu_9W_6**) compound.

compound	**5**	**Cu_9W_6**
	this work	*Inorg. Chem.*, 2015, **54**, 11049
empirical formula	$C_{138}H_{168}Co_1Cu_8N_{72}O_{18}W_6$	$C_{120}H_{168}Cu_9N_{72}O_{36}W_6$
formula weight	4793.78	4294.22
T, K	100(2)	173(2)
radiation	MoKα (λ = 0.71073 Å)	MoKα (λ = 0.71073 Å)
crystal system	triclinic	monoclinic
space group	P –1	P 2_1/n
a, Å	17.5625(7)	17.796(3)
b, Å	17.6025(8)	17.665(3)
c, Å	17.9412(7)	28.230(4)
α, deg	96.994(7)	90
β, deg	104.782(7)	91.778(2)
γ, deg	109.072(8)	90
V, Å^3	4939.1(5)	8870(2)
Z	1	2
ρ_{calc}, g/cm^3	1.612	1.608
qbs. coefficient, cm^{-1}	4.469	4.985
F(000)	2347	4194
crystal type	violet block	black block
crystal size, mm^3	0.13 × 0.12 × 0.08	0.22 × 0.20 × 0.18
θ range, deg	3.001 to 27.485	1.330 to 25.000
index range	$-22 \le h \le 22$, $-22 \le k \le 22$, $-21 \le l \le 23$	$-19 \le h \le 21$, $-20 \le k \le 20$, $-33 \le l \le 17$
reflections collected	68489	46330
independent reflections	22136	15226
R_{int}	0.1043	0.0579
completeness	0.977	0.975
data/restraints/ parameters	22136/135/1186	15226/314/1263
goodness-of-fit on F^2	1.090	1.040
final R indices [I >=2$\sigma(I)$]	R_1 = 0.1099, wR_2 = 0.2699	R_1 = 0.0448, wR_2 = 0.1196
R indices (all data)	R_1 = 0.1412, wR_2 = 0.2901	R_1 = 0.0738, wR_2 = 0.1107
largest diff. peak/hole, e·Å^{-3}	5.536/–6.024	2.176/–1.921

Table S7. Detailed structural parameters of **5** compared with the previously reported analogous $\{Cu^{II}[Cu^{II}(Me_3tacn)]_8[W^V(CN)_8]_6\}\cdot 5MeOH\cdot 31H_2O$ (**Cu_9W_6**) compound.

parameter	5	Cu₉W₆	parameter	5	Cu₉W₆
	this work (atom labels as in Fig. 2b and Fig. 3b)	*Inorg. Chem.*, 2015, **54**, 11049 (bond distances of the analogous complexes)		this work (atom labels as in Fig. 2b and Fig. 3b)	*Inorg. Chem.*, 2015, **54**, 11049 (bond distances of the analogous complexes)
Co1–N2	2.084(13) Å	Cu1, 1.950(7) Å	W1–CN	172.8(13)º to 179.0(14)º	175.2(7)º to 179.4(7)º
Co1–N14	2.080(12) Å	Cu1, 1.956(6) Å	W2–CN	174.6(17)º to 179.9(19)º	175.1(7)º to 179.0(16)º
Co1–N17	2.054(12) Å	-	W3–CN	172.4(14)º to 178.0(15)º	175.8(9)º to 179.1(10)º
Cu1–N8	2.059(15) Å	Cu4, 2.015(8) Å	W1–C1	2.164(15) Å	2.174(8) Å
Cu1–N13	2.291(14) Å	2.196(8) Å	W1–C2	2.154(15) Å	2.154(10) Å
Cu1–N20	2.038(14) Å	2.106(8) Å	W1–C3	2.158(15) Å	2.145(8) Å
Cu1–N25	2.234(17) Å	2.192(9) Å	W1–C4	2.149(17) Å	2.142(8) Å
Cu1–N26	2.127(16) Å	2.162(8) Å	W1–C5	2.124(19) Å	2.213(10) Å
Cu1–N27	2.070(16) Å	2.090(8) Å	W1–C6	2.160(17) Å	2.168(9) Å
Cu2–N3	2.396(14) Å	Cu3, 2.405(9) Å	W1–C7	2.200(19) Å	2.166(10) Å
Cu2–N15	2.012(14) Å	2.004(8) Å	W1–C8	2.159(17) Å	2.159(10) Å
Cu2–N18	2.012(15) Å	2.008(7) Å	W2–C9	2.177(18) Å	2.167(9) Å
Cu2–N28	2.085(15) Å	2.088(14) Å	W2–C10	2.18(2) Å	2.145(10) Å
Cu2–N29	2.294(14) Å	2.279(13) Å	W2–C11	2.136(15) Å	2.147(9) Å
Cu2–N30	2.075(14) Å	2.095(11) Å	W2–C12	2.148(18) Å	2.167(9) Å
Cu3–N4	2.030(13) Å	Cu5, 2.015(8) Å	W2–C13	2.160(19) Å	2.157(9) Å
Cu3–N12	1.989(13) Å	1.985(7) Å	W2–C14	2.136(19) Å	2.179(9) Å
Cu3–N24	2.370(15) Å	2.472(7) Å	W2–C15	2.151(14) Å	2.144(11) Å
Cu3–N31	2.114(14) Å	2.10(2) Å	W2–C16	2.098(16) Å	2.149(13) Å
Cu3–N32	2.290(15) Å	2.30(2) Å	W3–C17	2.136(16) Å	2.186(8) Å
Cu3–N33	2.059(15) Å	2.05(2) Å	W3–C18	2.176(15) Å	2.170(10) Å
Cu4–N1	2.000(13) Å	Cu2, 1.978(16) Å	W3–C19	2.165(12) Å	2.170(10) Å
Cu4–N16	2.381(16) Å	2.30(2) Å	W3–C20	2.148(16) Å	2.159(9) Å
Cu4–N19	2.031(14) Å	2.042(8) Å	W3–C21	2.178(16) Å	2.137(10) Å
Cu4–N34	2.096(12) Å	2.072(8) Å	W3–C22	2.156(15) Å	2.172(9) Å
Cu4–N35	2.298(15) Å	2.242(15) Å	W3–C23	2.16(3) Å	2.179(10) Å
Cu4–N36	2.095(11) Å	2.203(9) Å	W3–C24	2.15(2) Å	2.179(10) Å

Table S8. Results of Continuous Shape Measure (CSM) analysis for six- and eight-coordinated metal complexes in **5**.

metal complex	CSM parameters[a]			geometry
six-coordinated metal complexes				
-	OC-6	TPR-6	-	-
$[Co1(\mu\text{-}NC)_6]^{4-}$	0.015	16.599	-	OC-6
$[Cu1(\mu\text{-}NC)_3(Me_3tacn)]^{-}$	0.459	15.656	-	OC-6
$[Cu2(\mu\text{-}NC)_3(Me_3tacn)]^{-}$	0.740	15.115	-	OC-6
$[Cu3(\mu\text{-}NC)_3(Me_3tacn)]^{-}$	0.700	15.164	-	OC-6
$[Cu4(\mu\text{-}NC)_3(Me_3tacn)]^{-}$	0.699	15.821	-	OC-6
eight-coordinated metal complexes				
-	SAPR-8	TDD-8	BTPR-8	-
$[W1(CN)_8]^{3-}$	1.356	0.979	1.202	TDD-8
$[W2(CN)_8]^{3-}$	1.982	0.362	1.923	TDD-8
$[W3(CN)_8]^{3-}$	1.148	1.632	1.012	SAPR-8/BTPR-8

[a]CSM parameter represents the distortion from an ideal geometry. It equals 0 for an ideal polyhedron and increases with the increasing distortion. Polyhedrons used in calculations: OC-6 = parameter of an octahedron related to the O_h symmetry; TPR-6 = parameter of a trigonal prism related to the D_{3h} symmetry; SAPR-8 = parameter of a square antiprism geometry related to the D_{4d} symmetry; TDD-8 = parameter of a triangular dodecahedron related to the D_{2d} symmetry; BTPR-8 = parameter of a bicapped trigonal prism related to the C_{2v} symmetry.

References: (*a*) M. Llunell, D. Casanova, J. Cirera, J. Bofill, P. Alemany, S. Alvarez, M. Pinsky and D. Avnir, *SHAPE v. 2.1. Program for the Calculation of Continuous Shape Measures of Polygonal and Polyhedral Molecular Fragments*, University of Barcelona: Barcelona, Spain, 2013; (*b*) D. Casanova, J. Cirera, M. Llunell, P. Alemany, D. Avnir and S. Alvarez, *J. Am. Chem. Soc*., 2004, **126**, 1755.

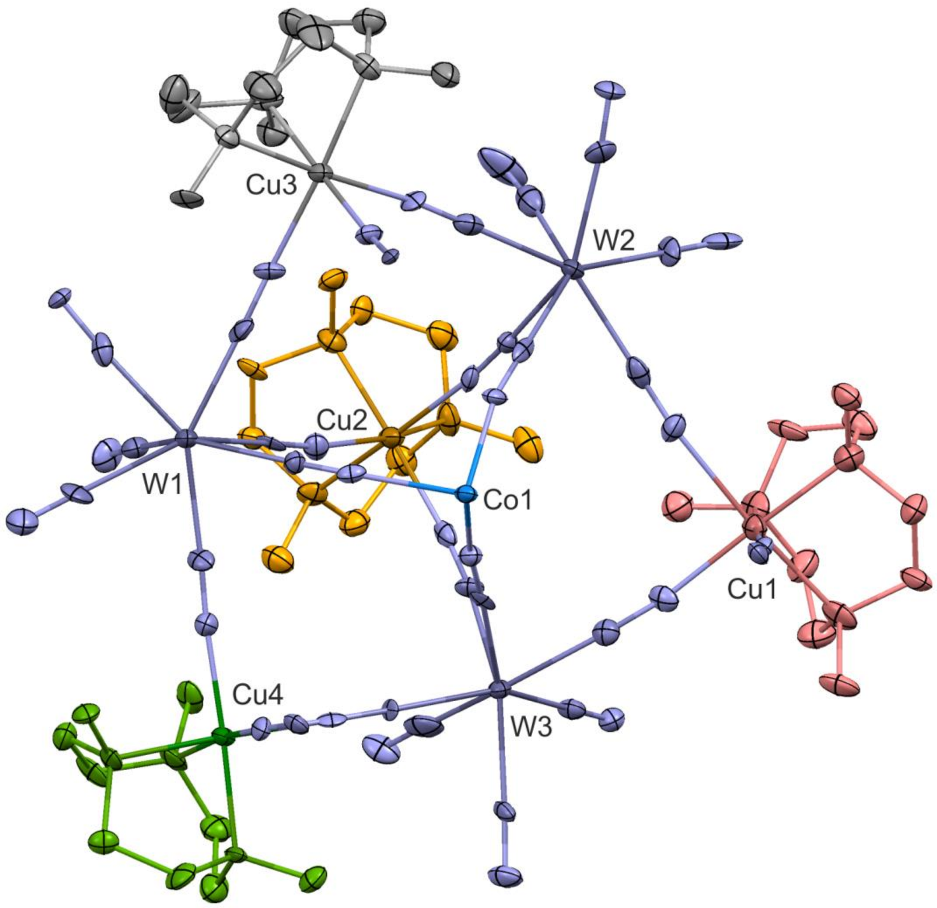

Figure S5. View of the asymmetric unit of **5** with the metal atoms labelling schemes. Thermal ellipsoids are presented at the 40% probability level. The detailed labelling scheme for the nitrogen atoms coordinated to Cu/Co metal centres is gathered in Figure 2b. The related bond lengths and angles are collected in Table S6. Hydrogen atoms are omitted for clarity.

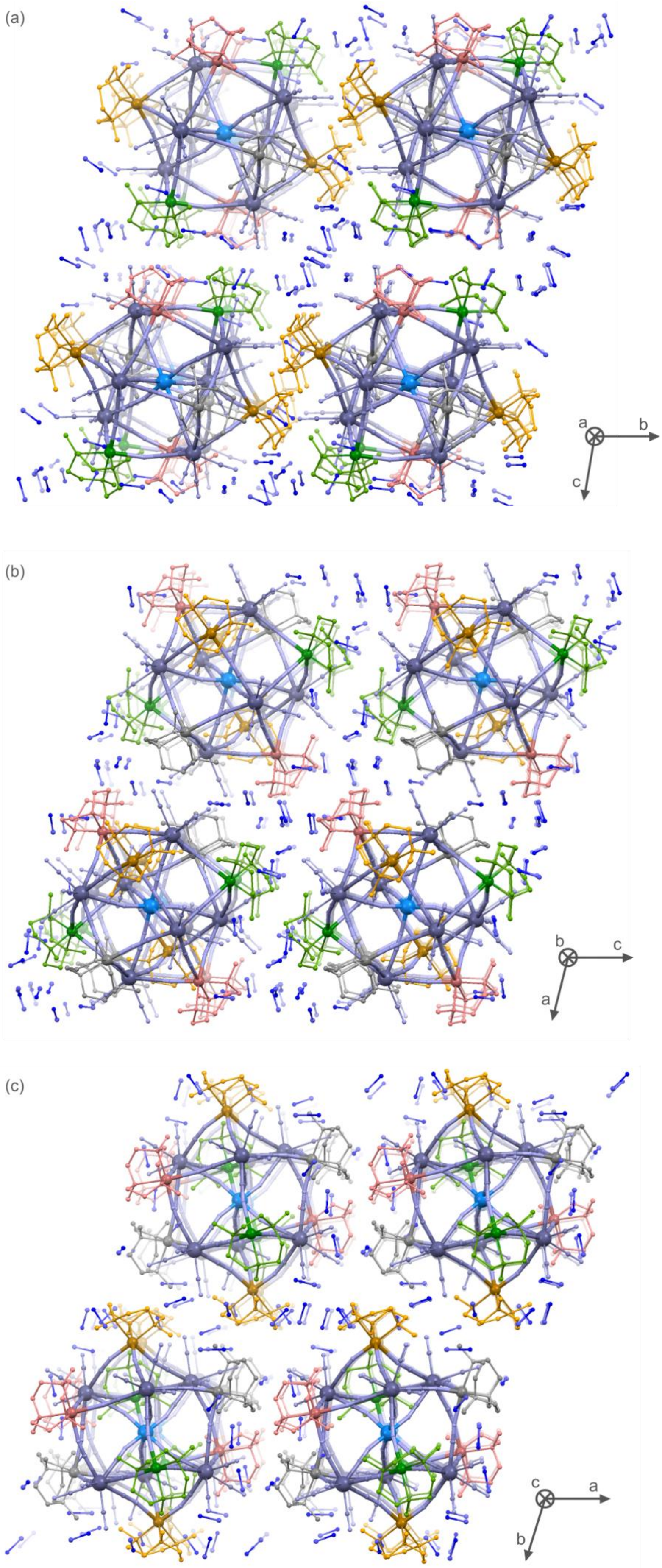

Figure S6. Views of the supramolecular network of **5** shown along the crystallographic ***a*** axis (a), ***b*** axis (b) and ***c*** axis (c). Atoms of clusters are coloured in the identical way as shown in Figure S5.

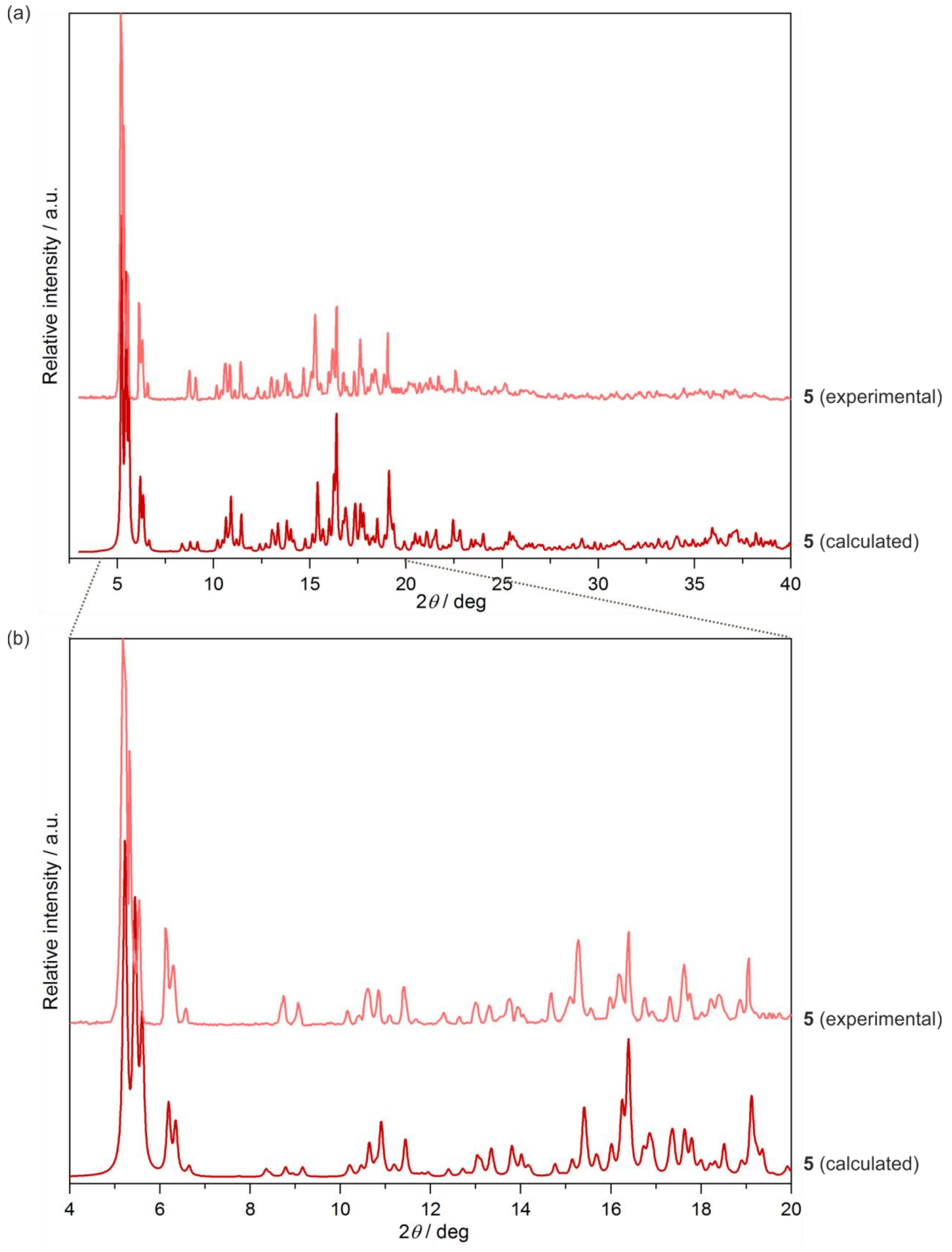

Figure S7. Experimental powder X-ray diffraction (PXRD) pattern of **5** presented in the broad 2*Θ* range of 2.5–40º (**a**) and in the limited low angle 2*Θ* range of 4–20º (**b**). In both cases, the experimental data were compared with the PXRD pattern calculated from the structural model obtained in the single-crystal X-ray diffraction structural analysis.

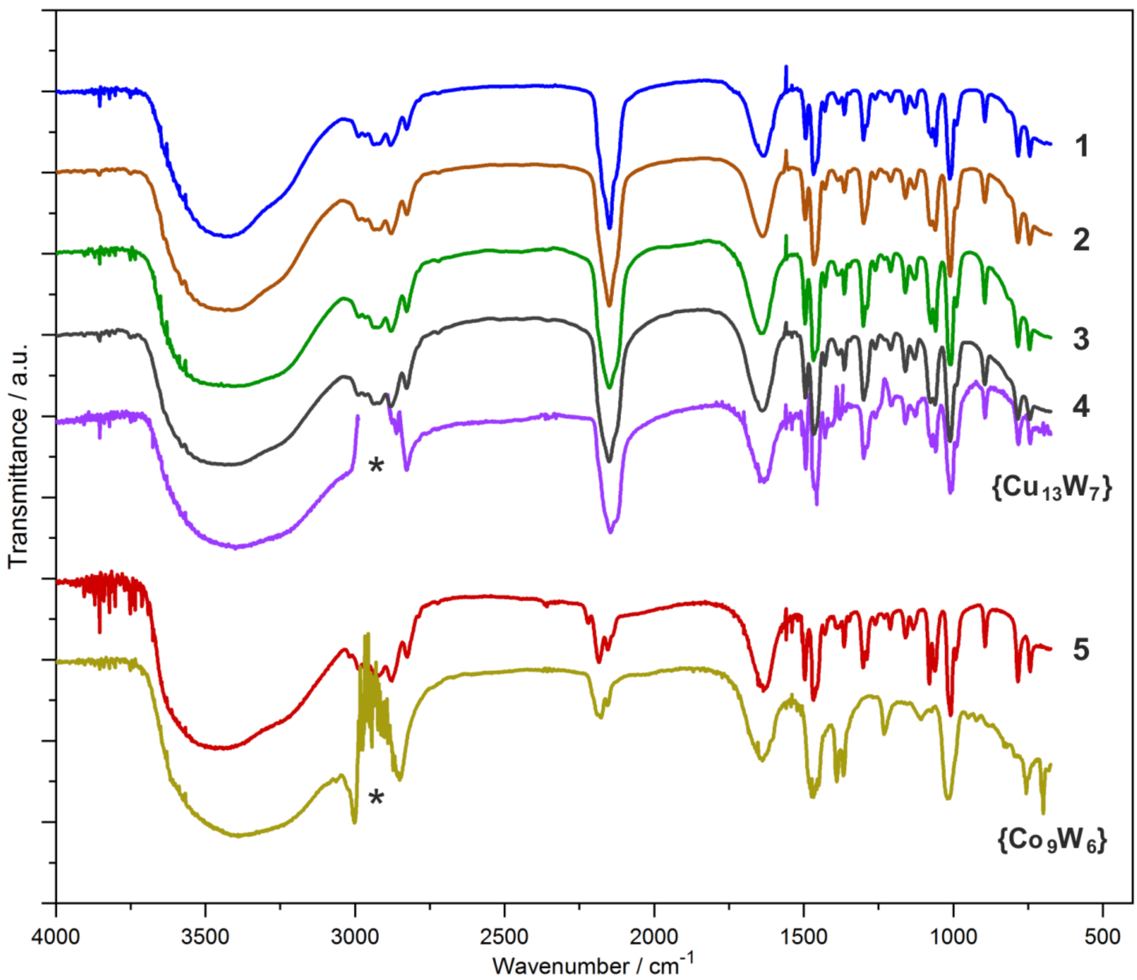

Figure S8. Infrared absorption spectra of **1**–**5** measured at room temperature for the selected single crystals in the 4000–700 cm^{-1} range, compared with the reference compounds of {[$Cu^{II}_{13}(Me_3tacn)_{12}(H_2O)$][$W^{IV}(CN)_8$]$_5$[$W^{V}(CN)_8$]$_2$}·24$H_2O$ (**$Cu_{13}W_7$**) (*Inorg. Chem.*, 2010, **49**, 3101) and {Co^{II}[$Co^{II}(MeOH)_3$]$_8$[$W^{V}(CN)_8$]$_6$}·19H_2O (**Co_9W_6**) molecules (*J. Am. Chem. Soc.*, 2005, **127**, 3708). The unusual discrepancies in the transmittance in the region of 3000–2800 cm^{-1} (marked with asterisk) are due to the absorption of NVH immersion oil used for protection of the crystals.

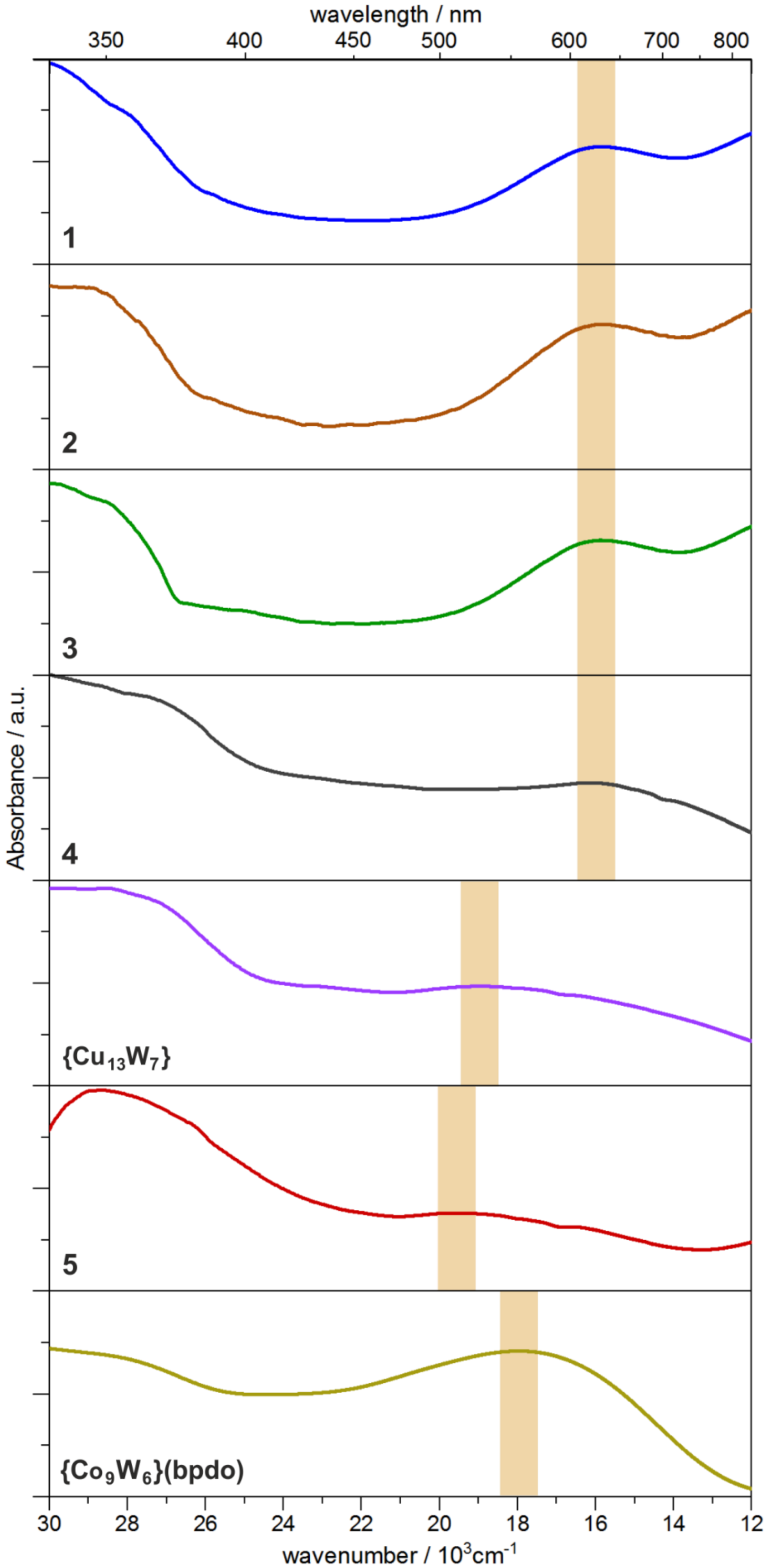

Figure S9. UV–vis absorption spectra of **1**–**5** measured at room temperature in the 30000–12000 cm^{-1} (333–833 nm) range, compared with the reference compounds of {[Cu$^{II}_{13}$(Me$_3$tacn)$_{12}$(H$_2$O)][W^{IV}(CN)$_8$]$_5$[W^{V}(CN)$_8$]$_2$}·24H$_2$O (**Cu$_{13}$W$_7$**) (*Inorg. Chem.*, 2010, **49**, 3101) and {Co$^{II}_9$(2,2'-bpdo)$_{6.5}$(MeOH)$_{11}$[W^{V}(CN)$_8$]$_6$}·8H$_2$O·2MeCN·27MeOH (**Co$_9$W$_6$-bpdo**) molecules (*Chem. Commun.*, 2016, **52**, 4772). The coloured boxes represent the frequency ranges of the main absorption maxima in the visible region: 610–650 nm for **1**–**4**, 515–540 nm for **Cu$_{13}$W$_7$**, 500–530 for **5** and 545–575 for **Co$_9$W$_6$-bpdo**.

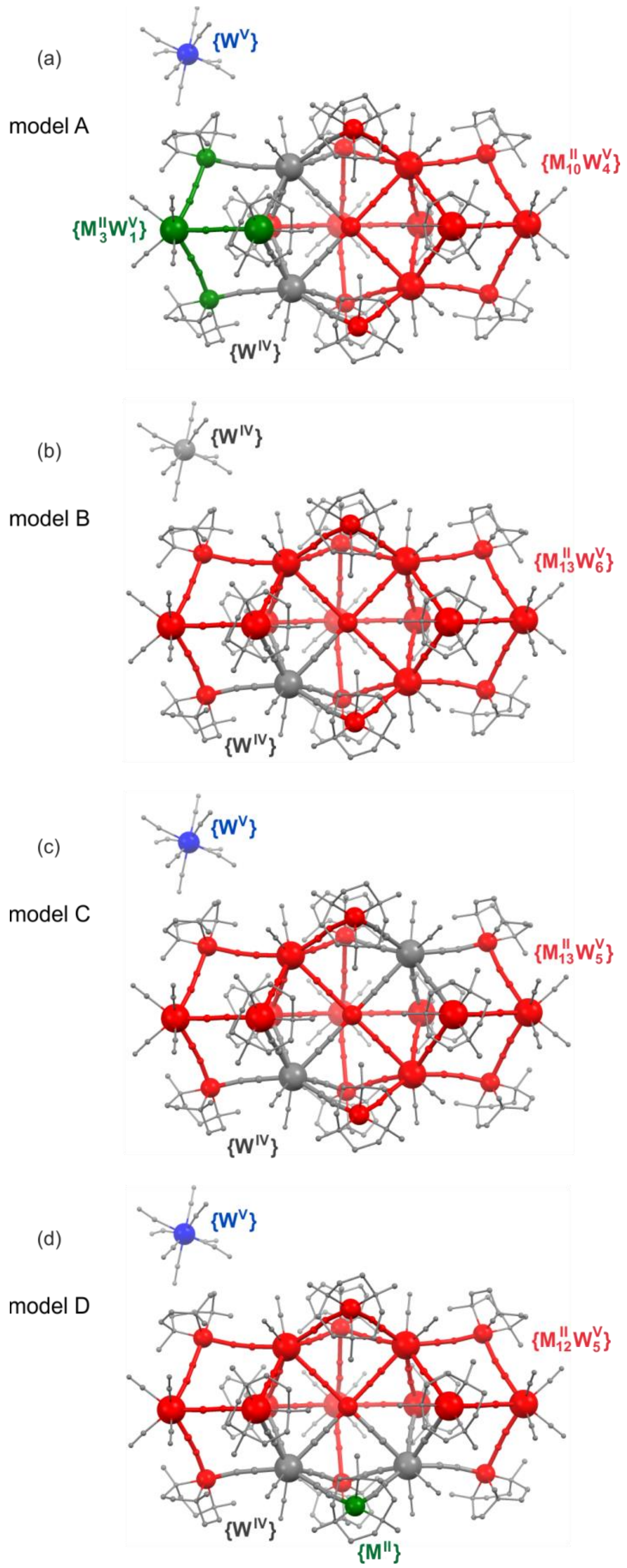

Figure S10. Four representative magnetic models analysed for the 20-centred cluster-based compounds **1**–**4**: (*a*) model A with two intracluster $\{M^{II}_{10}W^{V}_{4}\}$ and $\{M^{II}_{3}W^{V}\}$ magnetic units and additional $\{W^{V}\}$ magnetic counter-ion, (*b*) model B with $\{M^{II}_{13}W^{V}_{6}\}$ magnetic unit, (*c*) model C with $\{M^{II}_{13}W^{V}_{5}\}$ magnetic unit and $\{W^{V}\}$ magnetic counter-ion, (*d*) model D with $\{M^{II}_{12}W^{V}_{5}\}$ magnetic unit, separate $\{M^{II}\}$ magnetic centre and $\{W^{V}\}$ magnetic counter-ion. The resulting calculated values of maximal $\chi_M T$ product and saturation magnetization, M_S for the respective magnetic models are shown in Tables S9–S10.

Table S9. Predicted values of maximal $\chi_M T$ product and saturation magnetization, M_S for the respective magnetic models (Figure S10) analysed for the 20-centred cluster-based compound **2**.

compound 2, {$Ni_{1.5}Cu_{11.5}W_7$}+{W}, assuming ferromagnetic Ni–W and Cu–W interactions, S_{Ni} = 1, S_{Cu} = 1/2, S_W = 1/2, g_{Ni} = 2.2, g_{Cu} = 2.0, g_W = 2.0		S_{GS}	g_{av}	$\chi_M T$ [cm^{3}mol^{-1}K]	M_S [μ_B]
model A {$M^{II}_{10}W^{V}_{4}$}+{$M^{II}_{3}W^{V}_{1}$}+{W^V}					
Option A1 (12.5% probability)	{$Cu^{II}_{10}W^{V}_{4}$}	7	2.00	28.00	14
	{$Ni^{II}_{1}Cu^{II}_{2}W^{V}_{1}$}	2.5	2.05	4.6	5.12
	{W^V}	0.5	2.00	0.37	1
	sum	-	-	**32.97**	**20.12**
Option A2 (37.5% probability)	{$Ni^{II}_{1}Cu^{II}_{9}W^{V}_{4}$}	7.5	2.01	32.30	15.10
	{$Cu^{II}_{3}W^{V}_{1}$}	2	2.00	3.00	4
	{W^V}	0.5	2.00	0.37	1
	sum	-	-	**35.67**	**20.10**
Option A3 (25% probability)	{$Ni^{II}_{1}Cu^{II}_{9}W^{V}_{4}$}	7.5	2.01	32.30	15.10
	{$Ni^{II}_{1}Cu^{II}_{2}W^{V}_{1}$}	2.5	2.05	4.6	5.12
	{W^V}	0.5	2.00	0.37	1
	sum	-	-	**37.27**	**21.22**
Option A4 (25% probability)	{$Ni^{II}_{2}Cu^{II}_{8}W^{V}_{4}$}	8	2.03	37.09	16.24
	{$Cu^{II}_{3}W^{V}_{1}$}	2	2.00	3.00	4
	{W^V}	0.5	2.00	0.37	1
	sum	-	-	**40.37**	**21.24**
Average for model A		-	-	**36.91**	**20.65**
model B {$M^{II}_{13}W^{V}_{6}$}					
Option B1 (50% probability)	{$Ni^{II}_{1}Cu^{II}_{12}W^{V}_{6}$}	10	2.01	55.55	20.10
Option B2 (50% probability)	{$Ni^{II}_{2}Cu^{II}_{11}W^{V}_{6}$}	10.5	2.02	61.59	21.21
Average for model B		-	-	**58.57**	**20.65**
model C {$M^{II}_{13}W^{V}_{5}$}+{W^V}					
Option C1 (50% probability)	{$Ni^{II}_{1}Cu^{II}_{12}W^{V}_{5}$}	9.5	2.01	50.37	19.10
	{W^V}	0.5	2.00	0.37	1
	sum	-	-	**50.74**	**20.10**
Option C2 (50% probability)	{$Ni^{II}_{2}Cu^{II}_{11}W^{V}_{5}$}	10	2.02	56.11	20.20
	{W^V}	0.5	2.00	0.37	1
	sum	-	-	**56.48**	**21.20**
Average for model C		-	-	**53.61**	**20.65**
model D {$M^{II}_{12}W^{V}_{5}$}+{M^{II}}+{W^V}					
Option D1 (50% probability)	{$Ni^{II}_{1}Cu^{II}_{11}W^{V}_{5}$}	9	2.01	45.45	18.09
	{M^{II}} = {Cu^{II}}	0.5	2.00	0.37	1
	{W^V}	0.5	2.00	0.37	1
	sum	-	-	**46.19**	**20.09**
Option D2 (50% probability)	{$Ni^{II}_{2}Cu^{II}_{10}W^{V}_{5}$}	9.5	2.02	50.88	19.19
	{M^{II}} = {Cu^{II}}	0.5	2.00	0.37	1
	{W^V}	0.5	2.00	0.37	1
	sum	-	-	**51.62**	**21.19**
Average for model D		-	-	**48.91**	**20.65**
Experimental values (Figure 5b)		-	-	**30.09 (9.0 K)**	**20.08 (70 kOe)**

Table S10. Predicted values of maximal $\chi_M T$ product and saturation magnetization, M_S for the 20-centred cluster-based compounds **1** and **3** using the selected magnetic model A (Figure S10).

compound 1, {$Co_1Cu_{12}W_7$}+{W}, assuming ferromagnetic Co–W and Cu–W interactions, $S_{Co,eff,LT}$ = 1/2, S_{Cu} = 1/2, S_W = 1/2, $g_{Co,eff,LT}$ = 4.3, g_{Cu} = 2.0, g_W = 2.0		S_{GS}	g_{av}	$\chi_M T$ [$cm^3mol^{-1}K$]	M_S [μ_B]
Option CoF1 (25% probability)	{$Cu^{II}_{10}W^{V}_{4}$}	7	2.00	28.00	14
	{$Co^{II}_{1}Cu^{II}_{2}W^{V}_{1}$}	2	2.57	4.95	5.14
	{W^{V}}	0.5	2.00	0.37	1
	sum	-	-	**33.32**	**20.14**
Option CoF2 (75% probability)	{$Co^{II}_{1}Cu^{II}_{9}W^{V}_{4}$}	7	2.16	32.66	15.12
	{$Cu^{II}_{3}W^{V}_{1}$}	2	2.00	3.00	4
	{W^{V}}	0.5	2.00	0.37	1
	sum	-	-	**36.03**	**20.12**
Average for model A (ferro Co–W and Cu–W)		-	-	**35.35**	**20.13**
compound 1, {$Co_1Cu_{12}W_7$}+{W}, assuming antiferro- Co–W and ferromagnetic Cu–W interactions, $S_{Co,eff,LT}$ = 1/2, S_{Cu} = 1/2, S_W = 1/2, $g_{Co,eff,LT}$ = 4.3, g_{Cu} = 2.0, g_W = 2.0		S_{GS}	g_{av}	$\chi_M T$ [$cm^3mol^{-1}K$]	M_S [μ_B]
Option CoAF1 (25% probability)	{$Cu^{II}_{10}W^{V}_{4}$}	7	2.00	28.00	14
	{$Co^{II}_{1}Cu^{II}_{2}W^{V}_{1}$}	1	2.57	1.65	2.57
	{W^{V}}	0.5	2.00	0.37	1
	sum	-	-	**30.02**	**17.57**
Option CoAF2 (75% probability)	{$Co^{II}_{1}Cu^{II}_{9}W^{V}_{4}$}	6	2.16	24.49	12.96
	{$Cu^{II}_{3}W^{V}_{1}$}	2	2.00	3.00	4
	{W^{V}}	0.5	2.00	0.37	1
	sum	-	-	**27.86**	**17.96**
Average for model A (antiferro Co–W and ferro Cu–W)		-	-	**28.40**	**17.86**
Experimental values (Figure 5b)		-	-	**16.58 (4.0 K)**	**20.58 (70 kOe)**
compound 3, {$Mn_{1.5}Cu_{11.5}W_7$}+{W}, assuming antiferro- Mn–W and ferromagnetic Cu–W interactions, S_{Mn} = 5/2, S_{Cu} = 1/2, S_W = 1/2, g_{Mn} = 2.0, g_{Cu} = 2.0, g_W = 2.0		S_{GS}	g_{av}	$\chi_M T$ [$cm^3mol^{-1}K$]	M_S [μ_B]
Option MnAF1 (12.5% probability)	{$Cu^{II}_{10}W^{V}_{4}$}	7	2.00	28.00	14
	{$Mn^{II}_{1}Cu^{II}_{2}W^{V}_{1}$}	1	2.00	1.00	2
	{W^{V}}	0.5	2.00	0.37	1
	sum	-	-	**29.37**	**17**
Option MnAF2 (37.5% probability)	{$Mn^{II}_{1}Cu^{II}_{9}W^{V}_{4}$}	4	2.00	10.00	8
	{$Cu^{II}_{3}W^{V}_{1}$}	2	2.00	3.00	4
	{W^{V}}	0.5	2.00	0.37	1
	sum	-	-	**13.37**	**13**
Option MnAF3 (25% probability)	{$Mn^{II}_{1}Cu^{II}_{9}W^{V}_{4}$}	4	2.00	10.00	8
	{$Mn^{II}_{1}Cu^{II}_{2}W^{V}_{1}$}	1	2.00	1.00	1
	{W^{V}}	0.5	2.00	0.37	1
	sum	-	-	**11.37**	**10**
Option MnAF4 (25% probability)	{$Mn^{II}_{2}Cu^{II}_{8}W^{V}_{4}$}	1	2.00	1.00	2
	{$Cu^{II}_{3}W^{V}_{1}$}	2	2.00	3.00	4
	{W^{V}}	0.5	2.00	0.37	1
	sum	-	-	**4.37**	**7**
Average for model A (antiferro Mn–W and ferro Cu–W)		-	-	**12.62**	**11.25**
Experimental values (Figure 5b)		-	-	**14.53 (18 K)**	**12.95 (70 kOe)**

Table S11. Predicted values of maximal $\chi_M T$ product and saturation magnetization, M_S for the 20-centred cluster-based compound **4** using the selected magnetic model A (Figure S10).

compound 4, {$Fe_{1.5}Cu_{11.5}W_7$}+{W}, assuming ferromagnetic Fe–W and Cu–W interactions, S_{Fe} = 2, S_{Cu} = 1/2, S_W = 1/2, g_{Fe} = 2.2, g_{Cu} = 2.0, g_W = 2.0		S_{GS}	g_{av}	$\chi_M T$ [$cm^3 mol^{-1} K$]	M_S [μ_B]
Option FeF1 (12.5% probability)	{$Cu^{II}_{10}W^{V}_{4}$}	7	2.00	28.00	14
	{$Fe^{II}_{1}Cu^{II}_{2}W^{V}_{1}$}	3.5	2.05	8.27	7.18
	{W^{V}}	0.5	2.00	0.37	1
	sum	-	-	**36.64**	**22.18**
Option FeF2 (37.5% probability)	{$Fe^{II}_{1}Cu^{II}_{9}W^{V}_{4}$}	8.5	2.01	40.94	17.09
	{$Cu^{II}_{3}W^{V}_{1}$}	2	2.00	3.00	4
	{W^{V}}	0.5	2.00	0.37	1
	sum	-	-	**44.31**	**22.09**
Option FeF3 (25% probability)	{$Fe^{II}_{1}Cu^{II}_{9}W^{V}_{4}$}	8.5	2.01	40.94	17.09
	{$Fe^{II}_{1}Cu^{II}_{2}W^{V}_{1}$}	3.5	2.05	8.27	7.18
	{W^{V}}	0.5	2.00	0.37	1
	sum	-	-	**49.58**	**25.27**
Option FeF4 (25% probability)	{$Fe^{II}_{2}Cu^{II}_{8}W^{V}_{4}$}	10	2.03	56.60	20.30
	{$Cu^{II}_{3}W^{V}_{1}$}	2	2.00	3.00	4
	{W^{V}}	0.5	2.00	0.37	1
	sum	-	-	**59.97**	**25.30**
Average for model A (ferromagnetic Fe–W and Cu–W)		-	-	**48.59**	**23.70**
compound 4, {$Fe_{1.5}Cu_{11.5}W_7$}+{W}, assuming antiferro- Fe–W and ferromagnetic Cu–W interactions, S_{Fe} = 2, S_{Cu} = 1/2, S_W = 1/2, g_{Fe} = 2.2, g_{Cu} = 2.0, g_W = 2.0		S_{GS}	g_{av}	$\chi_M T$ [$cm^3 mol^{-1} K$]	M_S [μ_B]
Option FeAF1 (12.5% probability)	{$Cu^{II}_{10}W^{V}_{4}$}	7	2.00	28.00	14
	{$Fe^{II}_{1}Cu^{II}_{2}W^{V}_{1}$}	0.5	2.05	0.39	1.02
	{W^{V}}	0.5	2.00	0.37	1
	sum	-	-	**28.76**	**16.02**
Option FeAF2 (37.5% probability)	{$Fe^{II}_{1}Cu^{II}_{9}W^{V}_{4}$}	4.5	2.01	12.55	9.05
	{$Cu^{II}_{3}W^{V}_{1}$}	2	2.00	3.00	4
	{W^{V}}	0.5	2.00	0.37	1
	sum	-	-	**15.92**	**14.05**
Option FeAF3 (25% probability)	{$Fe^{II}_{1}Cu^{II}_{9}W^{V}_{4}$}	4.5	2.01	12.55	9.05
	{$Fe^{II}_{1}Cu^{II}_{2}W^{V}_{1}$}	0.5	2.05	0.39	1.02
	{W^{V}}	0.5	2.00	0.37	1
	sum	-	-	**13.31**	**11.07**
Option FeAF4 (25% probability)	{$Fe^{II}_{2}Cu^{II}_{8}W^{V}_{4}$}	2	2.03	3.09	4.06
	{$Cu^{II}_{3}W^{V}_{1}$}	2	2.00	3.00	4
	{W^{V}}	0.5	2.00	0.37	1
	sum	-	-	**6.46**	**9.06**
Average for model A (antiferro Fe–W and ferro Cu–W)		-	-	**14.51**	**12.30**
Experimental values (Figure 5b)		-	-	**24.60 (1.8 K)**	**22.13 (70 kOe)**